Study the Effects of Camera Mis-alignment on 3D Measurements for Efficient Design of Vision-based Inspection Systems

Deepak Dwarakanath[1 2 3], Carsten Griwodz[1 2],
Paal Halvorsen[1 2], and Jacob Lildballe[3]

[1] Simula Research Laboratory
Martin Linges vei 17/25, Lysaker 1325, Norway
{deepakd}@simula.no
[2] University of Oslo
Gaustadallen 23 B, N-0373 Oslo, Norway
{griff,paal}@ifi.uio.no
[3] Image House PantoInspect A/S
Carsten Niebuhrs Gade 10, 2, DK-1577 Copenhagen V, Denmark
jl@pantoinspect.com

Abstract. Vision based inspection systems for 3D measurements using single camera, are extensively used in several industries, today. Due to transportation and/or servicing of these systems, the camera in this system is prone to mis-alignment from its original position. In such situations, although a high quality calibration exists, the accuracy of 3D measurement is affected. In this paper, we propose a statistical tool or methodology which involves. a) Studying the significance of the effects of 3d measurements errors due to camera mis-alignment. b) Modelling the error data using regression models. c) Deducing expressions to determine tolerances of camera mis-alignment for an acceptable inaccuracy of the system. This tool can be used by any 3D measuring system using single camera. Resulting tolerances can be directly used for mechanical design of camera placement in the vision based inspection systems.

Keywords: Camera calibration, Vision based inspection systems, Camera mis-alignment and Regression models.

1 Introduction

With the advent of automation in all types of industries, manual intervention in the operations of machines is minimized. Nowadays, automatic inspection systems are used to inspect various types of faults or defects in several application areas such as sorting and quality improvements in food industry [11], [10], inspection of cracks in roads [4], crack detection of mechanical units in manufacturing industries [8], [9] and so on. Vision based inspection systems are increasingly growing with the advance in computer vision techniques and algorithms.

Typically, vision based inspection systems that inspect objects of interest and estimate measurements, are required to know a priori information about the intrinsic (focal length, principal axes) and the extrinsic (position and orientation) parameters of the camera without any freedom of scale. These parameters are obtained by a camera calibration process [3],[5]. Usually, calibration is carried out offline, i.e., before the system is deployed and thereafter the calibrated parameters are used to recover 3D measurements from the 2D image of the camera [12], [13] [14]. The quality of the camera calibration is an important factor that determines the accuracy of the inspection system.

Although the quality of calibration might be very high, it is difficult to guarantee highly accurate measurements, if the camera is physically mis-aligned from the position assumed during calibration. However, the transportation or installation can cause mis-alignment, e.g., due to wrong mounting during installation, due to ways of handling the system during maintenance or service etc. Consequently, the performance of the inspection system degrades.

A possible correction to this problem would be to re-position the camera, physically, to its calibrated position or to run the calibration process after deployment. It is very difficult to physically re-position the camera with high precision. Alternatively, it might also be difficult to recalibrate in some situations based on the location and accessibility of the installed system.

Therefore, it becomes important to understand the effects of the offset in cameras' position and orientation on inaccuracies. The significance of the inaccuracies depends on design (acceptable inaccuracy level) and the application of the system. So, an important question is: what is the maximum tolerable camera mis-alignment for an acceptable inaccuracy of the system? By answering this question, we will be able to design and operate the system better. When the tolerance limits of the camera mis-alignment are known, the mechanical design of the camera housing and fixtures will need to adhere to these tolerances to maintain the inaccuracy below an acceptable level. Also, by using an empirical model, it is possible to estimate the camera mis-alignment and further re-calibrate the camera parameters to increase the robustness of the system.

This paper aims to enhance the design and operational aspects of vision-based inspection systems. The main contribution of this paper is to provide a simple statistical method or tool which can compute acceptable tolerance values for positions and orientations in all directions for a given accuracy requirements. This tool is useful in designing the mechanics and in increasing the robustness of the vision based inspection system. It is easily implementable and reproducible. The limitation of this tool is that the measurements are carried out on points that are assumed to be lying on a plane. However, the tool is easily extendable to measure 3D points as long as an appropriate calibration process is carried out based on known 3D points. Related work is described in section 2.

First, we identify a suitable use case for the study of effects of camera mis-alignment on 3D measurements. One such vision based inspection system that exhibits a similar purpose and problems mentioned so far, is the PantoInspect system [2]. This system is explained in detail in section 3. Details of our exper-

imental design is explained in section 4. The simulation results and the empirically obtained regression model is explained in section 5. Finally the paper is concluded by summarising the goal and evidence of the paper.

2 Related work

The effects of mis-alignment of stereoscopic cameras are studied in [15], [16], however, in our case we study the effects due to mis-alignment of single cameras. [15] focusses on the effects of calibration errors on depth errors, and provides tolerances on calibration parameters. In [16], camera mis-alignment is estimated and corrected. In both the papers, the approaches rely strongly on a second image and errors of the cameras' orientation with respect to each other. Other papers only discuss effects of camera mis-alignment on calibration parameters itself [15], [17] and [18]. In our case, where we use a single camera, we assume that calibration is of sufficiently high quality, but once calibrated, the effects of camera mis-alignment due to certain factors requires more attention in practical systems and hence, we study this in our paper. Our approach leads to an estimation of tolerances for camera mis-alignment that aims directly at the mechanical design of single camera vision systems. One major feature of our approach is that it is not specific to one application, but can be used for any application of this type.

3 The PantoInspect System

PantoInspect is a fault inspection system, which inspects pantographs and measures the dimensions of the defects in their carbon strips. PantoInspect is installed, as shown in figure 1, over railway tracks to inspect trains running with electric locomotives that are equipped with pantographs. Pantographs are mechanical components placed on one or more wagons of the train, which can be raised in height so that they touch the contact wire for electricity. Pantographs have one or more carbon strips that are actually in contact with the wire. Over time, due to constant contact of carbon strips with the wire, and probably other factors, various types of defects (cracks, edge chips etc.) are seen. Such defects are detected by the PantoInspect system.

3.1 Principle

PantoInspect is mounted right above the train tracks on bridges or other fixtures. The PantoInspect system receives a notification when the train is approaching and prepares itself. When the train passes right below the system, three line lasers are projected onto the carbon strips (depicted as green line in the figure), and the camera captures the near infrared image of the laser. When defects are present, the line deforms instead of remaining a straight line in the image. Hence, the laser line defines the geometry of the defect. The system then analyses the images, measures the dimension of the defects and notifies the user with alarms on certain measurement thresholds.

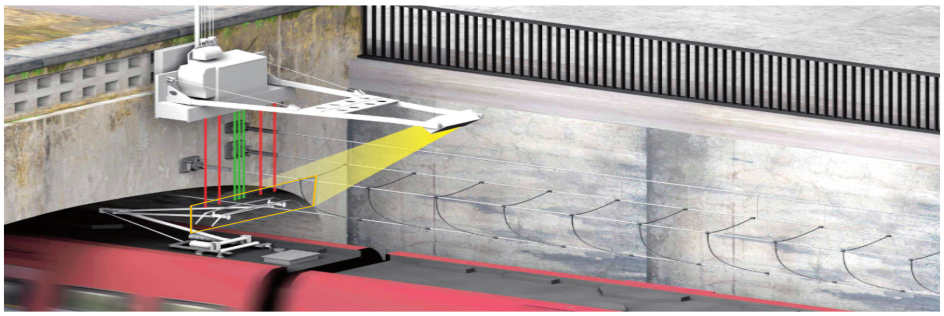

Fig. 1. PantoInspect system: inspects defects on the pantographs mounted on the trains.

The system measures various defects in the carbon strip based on the captured images. These defects are represented in figure 2, which are *(1)-thickness of carbon wear, (2)-vertical carbon cracks, (3)-carbon edge chips, (4)-missing carbon and (5)-abnormal carbon wear*. In general, all these defects are measured in terms of width and/or depth in real world metrics. Although the PantoInspect system measures various types of defects in pantographs, the common attribute in these measurements are width and depth. We therefore consider these attributes as the main 3D measurements in our scope of simulation and study of the effects of camera mis-alignment, in section 4.

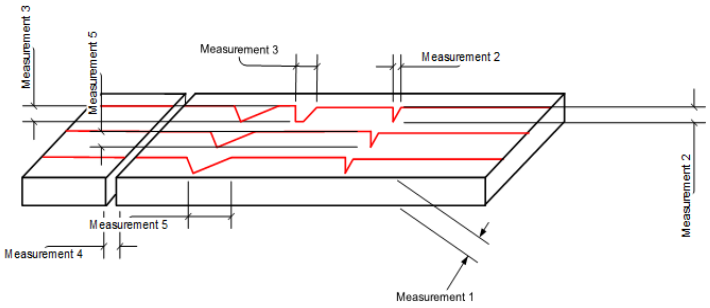

Fig. 2. Different carbon defects and the laser line deformations.

3.2 Calibration:

The system uses 2D pixel measurements in the image and estimates the real-world 3D scales. Camera calibration is an important step in obtaining such 3D measurements. For PantoInspect, this is carried out in the factory before

installing the system, using Bouguet's method [1]. A number of checkerboard images are used to estimate the intrinsic parameter K of the camera that constitutes focal length and principle axes of the camera. Next, a single image of the checkerboard that is placed exactly on the laser plane, is used to estimate the extrinsic parameter of the camera - position T and orientation R, with respect to the checkerboard coordinates.

3.3 Homography

In the scenario of PantoInspect system, we consider an imaginary plane passing vertically through the line laser as in figure 3. Then, the points representing defects are lying on a laser plane. These 2D points of the defects in the image are detected, and the conversion from 2D (p,q) to 3D (X,Y,Z) points becomes merely a ray-plane intersection [6], as shown in equation 1, where 3D and 2D points are expressed in homogeneous coordinates.

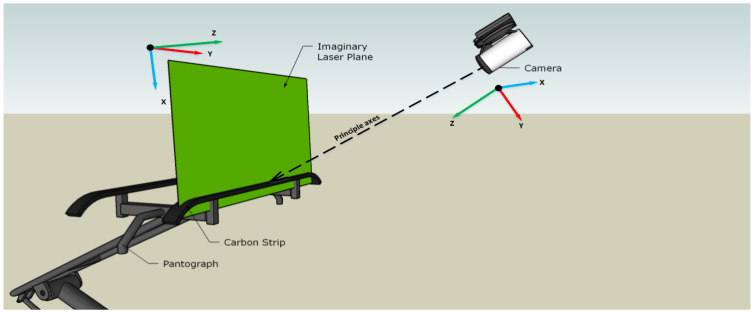

Fig. 3. Inspection scenario: world coordinates (Z=towards camera, Y=horizontal, X=vertical) and camera coordinates (Z=towards plane, Y=vertical, X=horizontal).

$$\begin{bmatrix} p \\ q \\ 1 \end{bmatrix} = K[R|T] \begin{bmatrix} X \\ Y \\ Z \\ 1 \end{bmatrix} \tag{1}$$

The K, R and T are obtained from the calibration process. The R matrix and the T vector are represented with their components in equation 2. Since 3D points are lying on the plane, the Z axis is zero. The rotation components in the 3rd column (r_{13}, r_{23}, r_{33}) are ignored because they are multiplied by zero.

$$\begin{bmatrix} p \\ q \\ 1 \end{bmatrix} = K * \begin{bmatrix} r_{11} & r_{12} & r_{13} & t_1 \\ r_{21} & r_{22} & r_{23} & t_2 \\ r_{31} & r_{32} & r_{33} & t_3 \end{bmatrix} \begin{bmatrix} X \\ Y \\ 0 \\ 1 \end{bmatrix} = \underbrace{K * \begin{bmatrix} r_{11} & r_{12} & t_1 \\ r_{21} & r_{22} & t_2 \\ r_{31} & r_{32} & t_3 \end{bmatrix}}_{H} \begin{bmatrix} X \\ Y \\ 1 \end{bmatrix} \tag{2}$$

Equation 2 describes a 2D-2D mapping between points on the image and points on the laser plane. This mapping is a homography (H). Using the homography, points on the plane can be recovered and measured for width and depth of defects that corresponds to defects detected in 2D pixel points.

4 Study methodology

We have seen how the camera parameters play an important role in estimating the measurements in PantoInspect. However when the camera is mis-aligned from its original position, estimated 3D measurements incur inaccuracies in the performance of the system. To study the effects of camera mis-alignment on 3D measurements, we carry out a simulation of the PantoInspect image analysis for 3D measurements, under the conditions of camera mis-alignment.

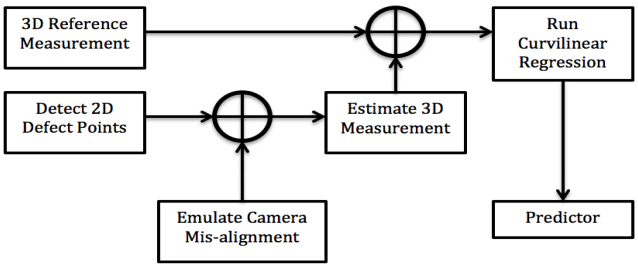

Fig. 4. Simulation procedure.

For repeatability of this simulation in any application involving 3D measurements of points lying on a plane and a single camera, a general procedure is shown in figure 4, followed by a specific explanation of the procedure for our case study.

4.1 Error computation

A set of points (P_w) that represents the crack edges on a plane are synthesized in the world coordinates. Note that the points are on the plane. Hence the Z axis is 0 for all points. These 3D points are synthesised using a random number generator. From these points, the width (W_{known}) and depth (D_{known}) of cracks are computed and recorded. These known measurements in 3D space are our baseline and used as a reference to evaluate the accuracy of the inspection.

The projection of the known set of points, P_w are computed based on the known camera parameters (K, R and T). These points represent the 2D points

(P_i) in image coordinates that are detected and further analysed by the PantoInspect system.

Typically, when the camera stays perfectly positioned and oriented, the width and depth of the cracks are measured with a reasonably good accuracy, due to high quality camera calibration process. To study the effects of camera mis-alignment on the accuracy of the measurements, the camera mis-alignment process needs to be emulated as if the camera had shifted position or orientation. Accordingly, points (P_i) are first represented in the camera coordinate system as P_{cam}, as depicted in equation 3. Next ,the rotation or translation effects are introduced, as a result of which the detected points obtain new positions, represented as $P_i^{misalign}$ in the image coordinates. Due to this emulation process that is based on changed camera orientation (R_{cam})and position (T_{cam}), the $P_i^{misalign}$ is estimated as in equation 4.

During inspection, the PantoInspect system detects measurable points (edges) of the cracks in the image and back-projects the 2D points into the 3D plane. The estimation of 3D points (P_w^{est}) of the crack is based on a pin-hole camera model and is mathematically shown in equation 5, where homography is a plane-plane projective transformation [6] as in equation 2.

$$P_{cam} = K^{-1} * P_i \tag{3}$$

$$P_i^{misalign} = K * \begin{bmatrix} R_{cam} & T_{cam} \\ 0^T & 0 \end{bmatrix} P_{cam} \tag{4}$$

$$P_w^{est} = H * P_i^{misalign} \tag{5}$$

Finally, the width (W^{est}) and depth (D^{est}) measurements are estimated and compared with the known values to compute the mean squared error, in equations 6 and 7. These errors $Error_{width}$ and $Error_{depth}$ represent the accuracy of the defect measurements.

$$Error_{width} = ||W - W^{est}||_2 \tag{6}$$

$$Error_{depth} = ||D - D^{est}||_2 \tag{7}$$

4.2 Prediction model

The simulation produces data pertaining to error in the 3D measurements with respect to camera mis-alignment in terms of three positional ($T_{cam} = [t_x, t_y, t_z]$) and three rotational ($R_{cam} = [r_x, r_y, r_z]$) mis-alignments. Considering each of these camera mis-alignment components as a variable, and the error as the response to it, the error can be modelled using appropriate regression models. Once the data fits to a model, the parameters of that model can be used for prediction purposes [7].

This is helpful to make predictions of camera mis-alignment based on the error estimated in the system. Then, given the acceptable accuracy of the system,

in terms of maximum allowable error in the measurements, one can deduce maximum limits or tolerances of camera mis-alignment to maintain an acceptable inaccuracy.

5 Simulation results

5.1 Priori

The carbon strip on each pantograph measures about 1.2meters in length and between 30-50mm in width and 30mm in thickness. For simulation purposes, we assume that there are about five defects per pantograph, and the system inspects about 200 such pantograph, i.e., 1000 measurements.

The defect width of maximum 50mm and defect depth of maximum 30mm are assumed to be present across the length of the carbon strip. The camera used for inspection is calibrated offline, and hence, a priori calibration data is available for that camera. The K, R and T matrices are as follows:

$$K = \begin{bmatrix} 4100.8633085 & 0 & 947.0315701 \\ 0 & 4104.1593558 & 554.2504842 \\ 0 & 0 & 1 \end{bmatrix}$$

$$R = \begin{bmatrix} 0.0108693 & 0.9999407 & -0.0006319 \\ 0.7647318 & -0.0079055 & 0.6443002 \\ 0.6442570 & -0.0074863 & -0.7647724 \end{bmatrix}$$

$$T = \begin{bmatrix} -540.7246414 & -119.4815451 & 2787.2170789 \end{bmatrix}$$

5.2 Effect of camera mis-alignment

The simulation procedure explained in section 4 is for one camera-plane pair, where a single camera calibration parameter (K, R, T, as given above) is used to recover the 3D measurements. We have conducted experiments on 6 such pairs. We used two different cameras, and each camera calibration with three planes corresponding to three line lasers. Results from all the 6 configurations yields similar patterns and are explained as follows.

For every such configuration, the simulation was carried over a range of camera's positional mis-alignment between -100mm to +100mm and orientational mis-alignment between -40 and +40 degrees. For every new position and/or orientation of mis-alignment, the simulation was carried out for 1000 measurements each.

The results of the simulation as in figure 5 and figure 6, show the variation in mean squared error of both the width and depth measurements for every camera mis-aligned position and orientation. This error represents the ability of the system to measure the inspected data accurately and error is measured in millimetres.

From figures 5(a) and 6(a), it can be seen that the camera translation t_x has the least effect on the errors compared to translations t_y and t_z. For insight into

the camera axes for translation and rotation please refer figure 3. The error for translations in t_y and t_z is higher, however, not significantly higher than 1mm, which might be an acceptable inaccuracy limit for certain applications. These effects are caused by the camera position mis-alignments, which shifts the back projected points, defining the width and depth measurements proportionally, so the relative width and depth measurements remain almost unchanged.

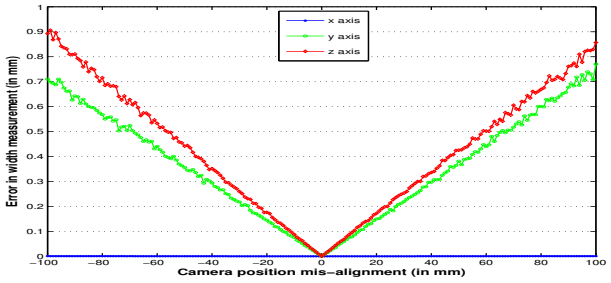

(a) Width error Vs camera position t_x, t_y, t_z

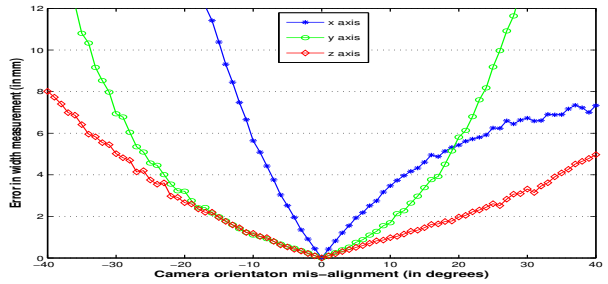

(b) Width error Vs camera orientation r_x, r_y, r_z

Fig. 5. Variation of error in 3D measurements (width) of the defects, due to changes in camera position and orientation about its camera centre.

Interesting effects are seen due to camera rotation, which has slightly different effects on width and depth. From figures 5(b) and 6(b), it can be seen that the camera rotations r_y and r_z, has noticeable effects on the width and depth errors. When the camera is rotated around axes y and z, the resulting 2D image point moves symmetrically within the image. Furthermore, the rate of increase of width is higher than depth for r_y, because when camera is rotated around the y axis, the horizontal component of the 2D point is changed more than the y component and width is a function of the x component. Exactly the opposite is seen when depth increases at higher rate for r_z, because depth is a function of the y component.

Special cases are the errors due to r_x. Remember that the camera is placed in a position to look down at the laser lines. The rotation around x axis will have a drastic projective effects in the image plane. The projective properties result in a non-symmetric variation of the errors around zero. One more thing to notice is that the error increases very quickly on the negative r_x than positive side. This behaviour can be explained using projective geometric properties. Consider an image capturing parallel lines and in perspective view, the parallel lines meet at vanishing (imaginary) point. It is possible to imagine that the width of parallel lines is shorter when the capturing device tilts downwards. Similarly when our camera is tilted downwards i.e. r_x in the positive (clockwise) direction, the defect points are moved upwards in the image plane, and the measurement becomes so small that the error seems to be constant. Contrarily, when the camera is tilted upwards, the detected points are moved downwards in the image plane, increasing the measurements and thereby the error.

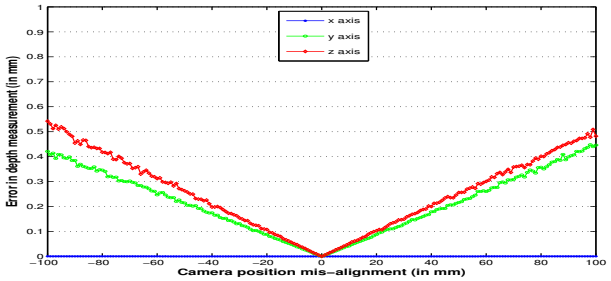

(a) Depth error Vs camera position t_x, t_y, t_z

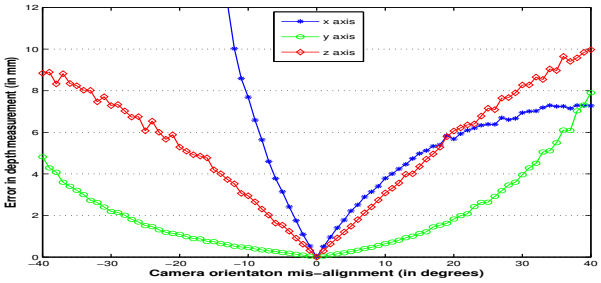

(b) Depth error Vs camera orientation r_x, r_y, r_z

Fig. 6. Variation of error in 3D measurements (depth) of the defects, due to changes in camera position and orientation about its camera centre.

5.3 Regression

By visual inspection of figures 5 and 6, we can say that errors are linearly varying with camera translations (t_x, t_y, t_z), and non-linear with camera rotations (r_x,

r_y, r_z). We not only model the data for every rotation and translation but also their direction (positive(+) and negative(-)). This means we separate out the error data for variables r_x^+, r_x^-, r_y^+, r_y^-, r_z^+, r_z^-, t_x^+, t_x^-, t_y^+, t_y^-, t_z^+ and t_z^-.

We model the emphirical data related to translations as a simple linear regression model and the data related to rotations are modelled as a curvilinear regression of degree 2. This results in the estimation of model parameters and gives rise to expressions for prediction.

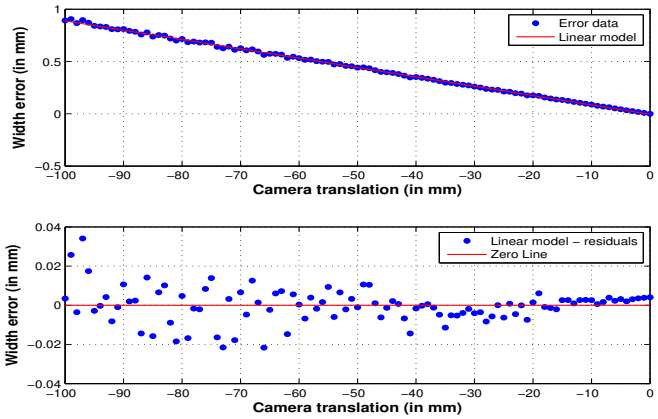

Fig. 7. Linear model fit and residual plots for width error data variation with t_z^-.

Figure 7 illustrates line fitting of variation in width due to t_z^- and figure 8 illustrates curve fitting of variation in depth due to r_y^+. Similarly all the data are modelled suitably well and the model parameters are estimated. An exhaustive list of parameters is shown in the table 1 and table 2.

Now, we have the model fitted to our data with root mean squared error (RMSE) less than unity values that implies good confidence level for estimation. The estimated model parameters are now used to deduce equations for prediction. Examples are shown in equations 8 and 9:

$$width = p0 + p1 * (t_z^-) \tag{8}$$

$$depth = p0 + p1 * (r_y^+) + p2 * (r_y^+)^2 + p3 * (r_y^+)^3 \tag{9}$$

5.4 Tolerance

Let us consider, in case of PantoInspect, the acceptable inaccuracy is 0.5mm. For this acceptable level of inaccuracy we can find the camera mis-alignment (rotation and position) based on the estimated model parameters. By solving

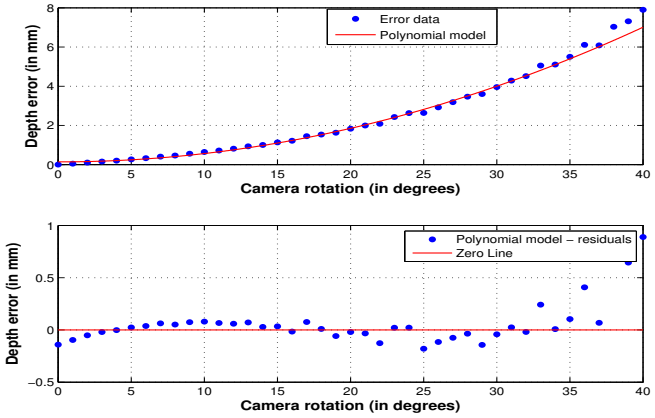

Fig. 8. Curvilinear (2 degree) model fit and residual plots for depth error data variation with r_y^+.

the equations defining the model for 0.5mm error, the maximum tolerance for the camera mis-alignments are estimated and are summarised as in table 3.

6 Conclusion

We identified the PantoInspect system as a suitable use case for measuring inspected data in 3D, using a single calibrated camera. To study the effects of camera mis-alignment on the accuracy of measurements, we emulated the camera mis-alignment in both position and orientation for several values, and obtained the width and depth error data. The resulting data was modelled using suitable regression models and we deduced expressions for prediction. Using the model parameters and expressions, we obtained tolerances for given acceptable inaccuracy limit.

Overall, our paper provided a statistical tool or a study methodology, that is easily implementable and reproducible. Our approach can be directly used by single camera vision systems to estimate tolerances of camera mis-alignment for an acceptable (defined) accuracy.

The knowledge about tolerance is helpful for mechanical design considerations of the camera placement in vision based inspection system, to achieve a desired level of confidence in the accuracy of the system. However, our approach assumes that the measurements are carried out on points that lie on a plane.

In the future, we would like to use the same model to estimate camera motion and further re-calibrate the camera on-the-fly, without the aid of the checkerboard.

Data	Linear		
f(x),x	p_0	p_1	RMSE
width, t_x^-	5.13e-07	-7.14e-06	6.36e-06
width, t_x^+	-1.73e-07	7.15e-06	5.47e-06
width, t_y^-	2.22e-03	-7.13e-03	6.47e-03
width, t_y^+	-1.28e-03	7.43e-03	6.41e-03
width, t_z^-	-4.04e-03	-8.93e-03	7.34e-03
width, t_z^+	3.84e-03	8.37e-03	7.20e-03
depth, t_x^-	5.09e-07	-4.23e-03	4.33e-06
depth, t_x^+	-6.48e-08	4.26e-06	3.51e-06
depth, t_y^-	1.54e-03	-4.23e-03	4.11e-03
depth, t_y^+	-2.7e-03	4.47e-03	4.118e-03
depth, t_z^-	-2.45e-03	-5.30e-03	5.62e-03
depth, t_z^+	1.77e-03	5.01e-03	3.83e-03

Table 1. Model parameters estimated for translation

Acknowledgement

We thank Lars Baunegaard With, Morten Langschwager and Claus Hoelgaard Olsen at Image House PantoInspect A/S, for all their valuable discussions and encouragement.

References

1. Bouguet, J.Y.: "Camera calibration toolbox for Matlab", (2008): *http : //www.vision.caltech.edu/bouguetj/calib_doc/*
2. Image House PantoInspect, Denmark: "*http : //www.pantoinspect.dk/*"
3. Zhengyou, Zhang: "A Flexible New Technique for Camera Calibration:IEEE Transactions on Pattern Analysis and Machine Intelligence":(1998): vol.22, p.1330-1334.
4. Aurélien, Cord, et. al.: "Automatic Road Defect Detection by Textural Pattern Recognition Based on AdaBoost": Comp.-Aided Civil and Infrastruct. Engineering: (2012): vol.27, No.4.
5. T Roger: "A Versatile Camera Calibration Technique for High-accuracy 3D Machine Vision Metrology using Off-the-shelf TV Cameras and Lenses": Robotics and Automation, IEEE Journal: (1987): 323-344.
6. R Hartley, Richard and Zisserman, Andrew:"Multiple View Geometry in Computer Vision":(2003):Cambridge University Press, isbn0521540518, ed.2, New York, USA.
7. J Raj: "The Art of Computer Systems Performance Analysis": John Wiley & sons inc.: (1991).
8. N S S Mar et.al.: "Design of Automatic vision Based Inspection System for Solder Joint Segementation": Journal of AMME: (2009): vol.34, issue 2.
9. Z Dongming, L Songtao: "3D Image Processing Method for Manufacturing Process Automation": Journal of Computing Industry: (2005): vol 56, no. 8.
10. T Brosnan et. al.: "Improving Quality Inspection of Food Products by Computer Vision - Review": Journal of Food Engineering 61: (2004): 3-16

Data	Polynomial			
f(x),x	p_0	p_1	p_2	RMSE
width, r_x^-	0.926	-0.014	0.064	0.912
width, r_x^+	-0.212	0.356	-0.005	0.142
width, r_y^-	0.688	0.095	0.011	0.468
width, r_y^+	0.974	-0.177	0.020	0.563
width, r_z^-	0.085	-0.072	0.003	0.102
width, r_z^+	0.127	0.065	0.001	0.076
depth, r_x^-	0.386	-0.235	0.029	0.394
depth, r_x^+	0.426	0.370	-0.005	0.141
depth, r_y^-	0.158	0.005	0.002	0.096
depth, r_y^+	0.140	-0.001	0.004	0.106
depth, r_z^-	-0.032	-0.319	-0.002	0.150
depth, r_z^+	-0.099	0.338	-0.002	0.130

Table 2. Model parameters estimated for rotations

Tolerances	X axis (deg/mm)	Y axis (deg/mm)	Z axis (deg/mm)
Rotation (width)	-0.46 to 0.82	-2.96 to 4.27	-4.73 to 5.12
Rotation (depth)	-0.11 to 0.19	-12.57 to 9.21	-1.68 to 1.79
Translation (width)	-6.97e04 to 6.98e04	-69.83 to 67.42	-56.41 to 59.20
Translation (depth)	-11.82e05 to 11.75e04	-117.93 to 112.35	-94.67 to 99.44

Table 3. Tolerances for camera mis-alignment, given the system inaccuracy limit as 0.5mm.

11. V G Narendra, K.S.Hareesh:"Quality Inspection and Grading of Agricultural and Food Products by Computer Vision - Review": IJCA: (2010).
12. T Heimonen, et. al.: "Experiments in 3D Measurements by Using Single Camera and Accurate Motion": Proceedings of the IEEE International Symposium: (2001):p.356,361.
13. S Wei, et. al.: "3D Displacement Measurement with a Single Camera based on Digital Image Correlation Technique": International Symposium on Advanced Optical Manufacturing and Testing Technologies: (2007): vol. 6723.
14. N Araki, et. al.: "Vehicle's Orientation Method by Single Camera Image Using Known-Shaped Planar Object": IJICIC: (2009): vol. 7, no. 7.
15. W Zhao and N, Nandhakumar: "Effects of Camera Alignment Errors on Stereoscopic Depth Estimates": Pattern Recognition, Elsevier: (1996): vol.29, p.2115-2126.
16. M , Santoro, et. al.:"Misalignment Correction for Depth Estimation using Stereoscopic 3-D Cameras": MMSP, IEEE 14th International Workshop: (2012): pp.19,24.
17. Godding et.al: "Geometric calibration and orientation of digital imaging systems.": Aicon 3D Systems, Braunschweig: (2002): http://www. falcon. de/falcon/eng/documentation.
18. H Eric, et.al.: "The Effects of Translational Misalignment when Self-Calibrating Rotating and Zooming Cameras.": Pattern Analysis and Machine Intelligence, IEEE Transactions: (2003): 1015-1020.